Influence of simplifications on FE modelling of mandible and TMJ implants

Girish Chandra[1], Vivek Verma[1,2], Rajdeep Ghosh[1,3,4], Kamalpreet Kaur[5], Ajoy Roychoudhury[5], Sudipto Mukherjee[1], Anoop Chawla[1], Kaushik Mukherjee[1, *]

[1]*Department of Mechanical Engineering, Indian Institute of Technology Delhi, New Delhi 110 016, Delhi, India.*

[2]*Department of Mechanical Engineering, Indian Institute of Technology Patna, Patna 801 106, Bihar, India*

[3]*School of Mechanical, Aerospace and Civil Engineering , University of Sheffield, Sheffield S1 3JD, United Kingdom*

[4]*Insigneo Institute, University of Sheffield, Sheffield S1 3JD, United Kingdom*

[5]*Department of Oral & Maxillofacial Surgery CDER, All India Institute of Medical Sciences, New Delhi 110029, Delhi, India*

*Corresponding author:

Dr. Kaushik Mukherjee

Department of Mechanical Engineering

Indian Institute of Technology Delhi

New Delhi, 110 016

Tel: +91 – 11-2654-8710

Email: kmukherjee@mech.iitd.ac.in

Keywords: *Mandible, Mandibular Implant, Biomet Stock TMJ, Mastication cycle; FE Analysis*

Number of Tables: 1; Number of Figures: 8

Appendix: Number of Tables: 1; Number of Figures: 3

Abstract

End-stage temporomandibular joint (TMJ) disorder often requires for replacement of TMJ for restoring bilateral mastication. Patient-specific TMJ implants often require detailed *in-silico* modelling based on subject-specific computed tomography (CT) scans of mandibles. However, creating these detailed finite element (FE) models is time-consuming and laborious due to segmentation of multiple components to appropriately capture the anatomical structure. Although it is known that any simplifications in the structure of mandible would influence its overall mechanical behaviour, influence of such modelling simplifications on TMJ implant design has hardly been investigated. Hence, this study investigates the biomechanical implications of following three model simplifications for intact and implanted mandibles: a detailed segmented mandible with tissue-specific material properties (Model 1), a simplified mandible made of cortical bone only (Model 2), and a further simplified mandible with dental crowns being excluded and made of cortical only (Model 3). For implanted mandible models, both narrow and standard TMJ implants were considered under both osseointegrated and non-osseointegrated conditions. Thus, a total of 15 FE models of intact (three) and implanted (12) models were developed. Physiological clenching activities were considered and the mechanical behaviour of intact and implanted mandibles were evaluated. Results revealed an overall reduction of 22-49% in principal stress, 16-50% in principal strain on bone and up to 79% in von Mises stress in TMJ implants in the biomechanically simplified model compared to the detailed segmented mandible model. It emphasizes the critical role of detailed mandible segmentation and material modelling to obtain reliable biomechanical evaluations of TMJ-TJR procedures.

1. Introduction

Temporomandibular joint facilitates essential functions such as mouth opening/closing, clenching/biting, and speaking. In a healthy human, these masticatory activities can go up to 1 million times annually (Nakhaei et al., 2023). In addition, the mandible has several important functions, being directly related to respiration, enunciation, and deglutition, and is also related to an individual's aesthetic (Al-Ahmari et al., 2015; Kim & Donoff, 1992; Luo et al., 2017; Seol et al., 2014). However, approximately 5% of the human population experience limitations in these activities due to end-stage TMJ disorders such as ankylosis (Balon et al., 2019; Ingawalé & Goswami, 2009). Total joint replacement (TJR) using TMJ implants is typically done to treat these conditions (Gonzalez-Perez et al., 2020; Yoda et al., 2020).

With the recent advancement in 3D printing and rapid prototyping (REFERENCE), the latest focus is on the design and development of patient-specific TMJ implants (REFERENCE). Designing patient-specific TMJ implants often warrants for detailed *in silico* evaluation to estimate post-operative biomechanical performances of these implants under masticatory loading (Banerjee et al., 2023; Deshmukh et al., 2012; Ingawale & Goswami, 2022; Kashi et al., 2010; Pinheiro et al., 2021; Vignesh et al., 2020). Most of these studies (INCLUDE REFERENCES) developed detailed FE models of mandible, with components like enamel, dentin, periodontal ligament, cancellous and cortical region and analyzed the implant performance under masticatory loading. On the contrary, there are multiple studies which simplified the FE model of mandible either by neglecting dentures (H. L. Huang et al., 2015; Oguz et al., 2009) or by considering entire mandible to be made of cortical bone (Filardi, 2020; C. M. Huang et al., 2021; Kharmanda & Kharma, 2017; Mesnard et al., 2011; Wang et al., 2017). However, there is no comparative study investigating

influences of such geometric and material simplifications on the biomechanical and load carrying performance of mandible and TMJ implant.

Hence, this study investigates the biomechanical implications of following three model simplifications for intact and implanted mandibles: a detailed segmented mandible with tissue-specific material properties (Model 1), a simplified mandible made of cortical bone only (Model 2), and a further simplified mandible with dental crowns being excluded and made of cortical only (Model 3). For implanted mandible models, both narrow and standard TMJ implants (45 mm long, Zimmer Biomet Microfixation system, Jacksonville, FL, USA) were considered under both osseointegrated and non-osseointegrated conditions. Thus, a total of 15 FE models of intact (three) and implanted (12) models were developed to understand the influence of mandible simplifications on stresses and strains in mandible and TMJ implants under masticatory loading.

2. Materials and Methods

Clinical CT images (512 x 512 pixels; pixel size of 0.439 mm; slice thickness of 0.75 mm) of a healthy 20-years-old male subject were acquired. Necessary ethics approval for this study was provided by the Institute Ethics Committee of AIIMS, New Delhi, India (IEC-611/15.07.2022, AA-3/05.08.2022, RP-11/2022). CT-specific mandible was developed in Materialise Mimics v25.0 (Materialise Inc., Leuven, Belgium) and meshed in Hypermesh v2022 (Altair Engineering Inc., Troy, MI, USA). Further FE-based biomechanical evaluations were performed in ANSYS Mechanical APDL v2022 R2 (ANSYS Inc., Canonsburg, PA, USA). Details of the FE model development process are being presented in subsequent sections.

2.1 Development of Intact Mandible Model

The subject-specific detailed intact mandible model (Model 1, Figure 1-b) was from our previous study (Ghosh et al., 2024). The model had multiple components including cortical, cancellous, teeth, periodontal ligament (PDL), articular fibrocartilage, and temporal bone blocks being segmented from the subject-specific CT data. Each component was assigned with tissue-specific material properties (Ghosh et al., 2024). Further details of model generation procedure are described in our previous study (Ghosh et al., 2024).

A simplified model of intact mandible (Model 2, Figure 1-c) was derived from this detailed mandible by neglecting separate segmentation of cancellous bone, PDL and teeth. Instead, the entire mandible (cortical, cancellous, PDL and teeth) was assumed to be made of cortical bone. The model, however, had articular fibrocartilage on its condyle and the temporal bone blocks. Thus, Model 2 reflected a mandible with simplified material properties. A further simplified model of intact mandible (Model 3, Figure 1-e) was derived from Model 2 only by excluding the dental crowns. All these mandibular models were discretized adaptively with quadratic tetrahedral elements having a range of edge length of 0.3 – 2 mm (Figure 2) based on the mesh convergence study performed earlier (Ghosh et al., 2024).

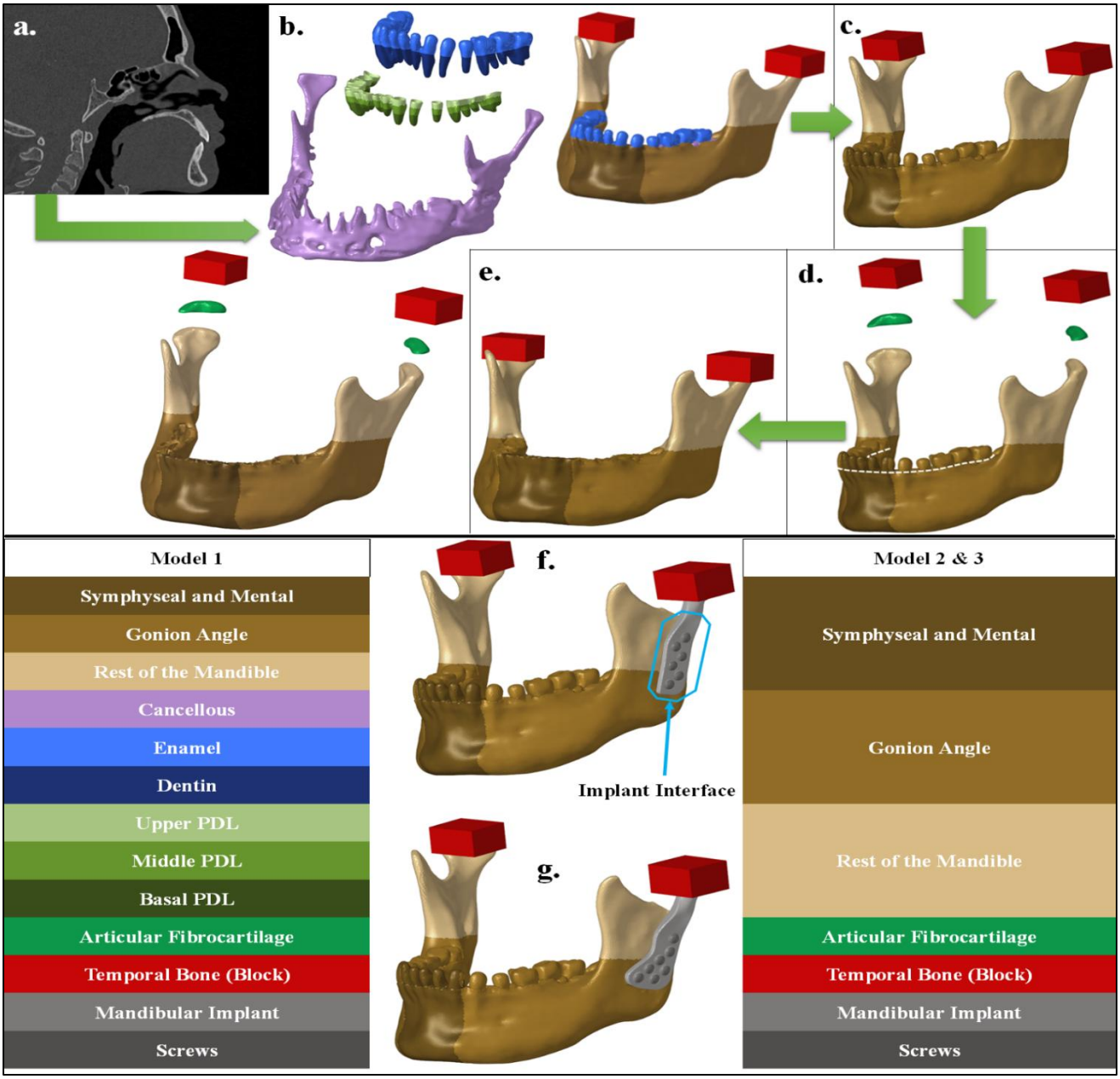

Figure 1. (a) CT data of an anonymous subject, (b) exploded view of detailed intact mandible model (Model 1) with its components, (c) simplified intact mandible model (Model 2) developed from Model 1, (d) exploded components view of the simplified intact mandible model (Model 2) showing crowns of teeth (above white dashed line) to remove for Model 3, (e) simplified intact mandible model (Model 3) with removed crown of teeth from Model 2, (f) osteotomized simplified mandible (Model 2) with attached components and narrow TMJ implants showing implant interface region, and (g) osteotomized mandible (Model 2) with attached components and standard TMJ implants

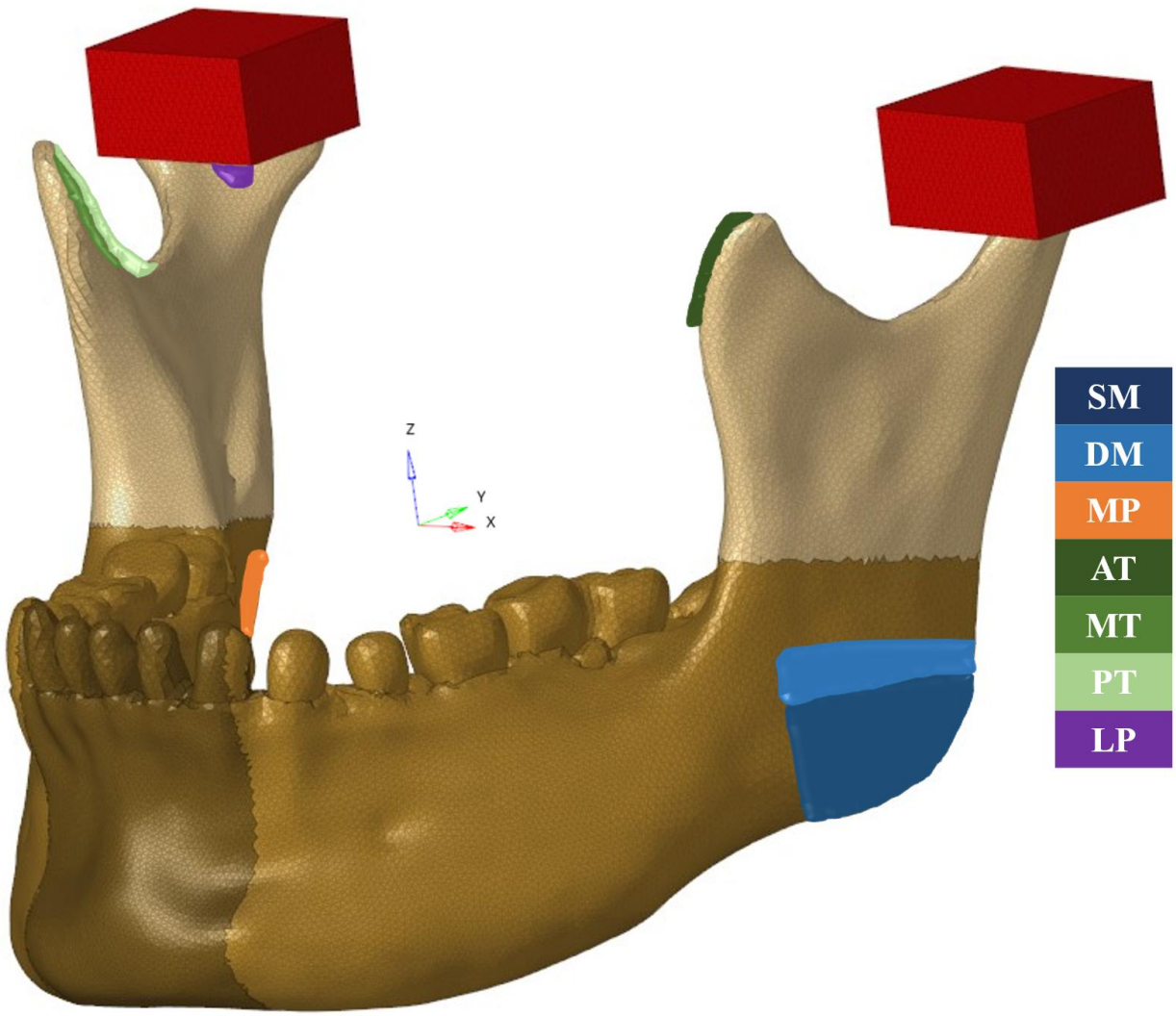

Figure 2. Different muscle locations (SM: Superior Masseter, DM: Deep Masseter, MP: Medial Pterygoid, AT: Anterior Temporalis, MT: Middle Temporalis, PT: Posterior Temporalis, LP: Lateral Pterygoid) considered in the FE models

2.2 Development of Implanted Mandible Models

The 3D models of Biomet narrow and standard mandibular stock implant components of size 45 mm (Zimmer Biomet Microfixation system, Jacksonville, FL, USA; Figure 1 - f & g) were obtained from micro-CT imaging (Xtreme CT II, Scanco Medical, Switzerland, isotropic voxel size: 60 μm). Based on Biomet mandibular screws (BIOMET Microfixation, 2007), bi-cortical

screws were modelled using SolidWorks 2022 (Dassault Systems, Vélizy-Villacoublay, France) as cylinders (Φ2.7 mm, length: 8 mm – 12 mm). The models of the intact mandible and TMJ implant were assembled into Rhinoceros® (Rhinoceros V7.0, Robert McNeel & Associates, Seattle, USA) for virtual implantation based on clinical recommendations. Based on our previous study (Ghosh et al., 2024), a suitable mesh size of ~ 0.5 mm edge length was used to discretize the TMJ implants. For each intact mandible model (three models: Model 1, Model 2 and Model 3), corresponding implanted models were developed with two types of stock TMJ implants (Narrow and Standard). Thus, six implanted mandible models were developed viz. first two having detailed mandible (Model 1) implanted with narrow and standard TMJ implants; second two having simplified mandible (Model 2) implanted with narrow and standard TMJ implants; last two having further simplified mandible (Model 3, without crown of teeth) implanted with narrow and standard TMJ implants.

2.3 Bone-Implant interface conditions

This study also investigated the combined influence of bone-implant interface conditions and anatomical simplification to understand the stress-strain distribution on the bone and implant. To simulate an osseointegrated (OI) interface condition, a bonded bone-implant interface was considered between the mandibular component and the cortical bone, whereas a frictional interface was used to replicate the non-osseointegrated (NOI) bone-implant interface. In addition, a frictional interface was also modelled between the fibrocartilage layer and the mandibular condyle. The interface between the head (uppermost region) of the mandibular component and the temporal bone was also considered frictional in the implanted mandible (Ghosh et al., 2024). All other interfacial contact pairs were considered bonded. With $\mu = 0.3$, an "Augmented Lagrangian Algorithm" was used to model every pair of surface-to-surface frictional contacts.

Biomechanical evaluation was conducted on 12 implanted models, incorporating both narrow and standard TMJ implants under OI and NOI conditions. These models were categorized as follows: first four models based on Model 1 from our previous study for comparison; the next four models with Model 2; and the final four models with Model 3.

2.4 Material properties

In our previous study with Model 1 (Ghosh et al., 2024) involving cortical, cancellous, PDL, and teeth, tissue-specific material properties (linear elastic) were chosen for each segmented (including the region-specific sub-divided segments (Korioth et al., 1992)) tissue layer. In the present study (Model 2 and Model 3) compared to our previous study (Model 1), the region-specific orthotropic material properties (Korioth et al., 1992) of cortical bone were considered to model the entire mandible including other anatomical tissue layers (cancellous, teeth, and PDL) for Model 2 and Model 3. Other than the mandible, material properties (linear elastic) of all other components such as articular fibrocartilage, temporal bone, and implants were considered isotropic same as our previous study. TMJ implants were assumed to be of Ti-alloy (Ti-6Al-4V) Medical Grade 23 ELI. Material properties of these region-specific cortical, associated components of the mandible and TMJ implants are listed in Table 1 for both Model 2 and Model 3 of the present study.

Table 1. Material properties of the components of the FE models (Korioth et al., 1992).

Components	Young's Modulus (GPa)			Poisson's Ratio			Shear Modulus (GPa)		
	E_x	E_y	E_z	ν_{xy}	ν_{yz}	ν_{xz}	G_{xy}	G_{yz}	G_{xz}
Cortical									
Symphyseal and mental	23	10	15	0.3	0.3	0.3	4.8	3.6	6.2
Gonial angle	20	11	12	0.3	0.3	0.3	4.8	5.3	6.0
Rest	17	6.9	8.2	0.3	0.3	0.3	2.8	2.9	4.6
Articular Fibrocartilage	0.006			0.47			-		
Mandibular component/screws (Ti-6Al-4V: ELI)	113.8			0.342			-		
Block (Temporal Bone)	Rigid			Rigid			-		

2.5 Loading and Boundary Conditions

Six clenching load cases (Appendix Table 1) were considered in the present study to simulate complete mastication cycle: incisal (INC), intercuspal (ICP), right molar (RMOL), left molar (LMOL), right group (RGF), and left group (LGF) bites (Ghosh et al., 2024), (Dutta et al., 2023; Hijazi et al., 2016). These tasks fall majorly in three categories: central (INC), unilateral (RMOL, LMOL, RGF and LGF) and bilateral (ICP). Muscle forces from primarily seven muscles (Figure 2) (Hijazi et al., 2016) namely, two masseters (SM/DM), two pterygoids (MP/LP), and three temporalis (AT/MT/PT) muscles were considered in the present study. However, the effect of the lateral pterygoid on the implanted side was ignored due to the removal of the condyle

(attachment site of lateral pterygoid). Furthermore, the current study also hypothesized the effective reattachment of all muscles post-surgery. The top surface of *os temporale* was fully constrained (Hijazi et al., 2016; Korioth et al., 1992). The displacements at bite points (the uppermost region on teeth) corresponding to each clenching task were restrained in Z-direction (Pinheiro et al., 2021).

2.6 Interpretation and verification of FE results

Erstwhile studies considered peak principal strains as a failure criterion for brittle cortical bones. (Fan et al., 2023; Schileo et al., 2008). As a result, in the current investigation, peak principal strains and stresses in the bone were used to compare the biomechanical behaviour of intact and reconstructed mandibles. To avoid stress and strain singularity which might arise due to the constrained and complicated anatomical regions in the FE models, 99th percentile principal stresses and strains on bone were reported in this study. In contrast, because of the ductile (Ti-6Al-4V ELI) behaviour of the implants, von Mises stress is used to investigate load transfer through the TMJ implants. The legends representing the contour plots of von Mises stresses on implants are chosen based on failure limit of the Ti-alloy (medical grade 23) where the yield strength and endurance limits are about 800 MPa and 500 MPa (for up to 10^7 cycles), respectively (Carrion et al., 2017).

The finite element (FE) results were verified following the methodology described in our previous work (Ghosh et al., 2024) and were benchmarked against findings from earlier studies (Gröning et al., 2013; Korioth et al., 1992; Meyer et al., 2002) to ensure consistency and reliability.

3. Results

In context of the study for biomechanical evaluation, a comparison is performed between the three different models (detailed mandible, Model 1, full cortical mandible, Model 2; and decrowned teeth full cortical mandible, Model 3). First, the principal stress and strain distributions across the bone are analyzed and discussed for intact and reconstructed mandibles, across different clenching tasks. Then the obtained equivalent von Mises stress in mandibular components and screws are discussed. The results obtained from the FE models developed in this study (Model 2 and 3) are then compared with the very accurate detailed segmented mandible (Model 1) which comprised all relevant anatomical details, including cortical bone (divided into three zones), cancellous bone, enamel, dentin and upper, middle, and basal root third periodontal ligament (Ghosh et al., 2024).

3.1 Biomechanical evaluation of mandible

3.1.1 Principal Stresses on mandible

Figure 3 shows the principal stress distribution in intact as well as implanted mandibles (with narrow and standard mandibular components) under the ICP biting case due to observed higher severity than other biting cases from our previous study (Ghosh et al., 2024) . All biting cases are shown in Appendix Figure 1 for principal stress distribution. The principal stress was observed between 3-10 MPa during all six loading conditions of the complete mastication cycle as shown in Figure 4. The upper bound of principal stresses was consistently observed in the ICP (max. 9.45 MPa) load case. The lower bounds of principal stresses were seen under group function biting conditions, with a maximum value of 4.57 MPa observed for both narrow and standard implanted mandibles. For intact mandibles, the lower bounds were recorded under LGF condition. The stress differences between RGF and LGF conditions across intact and implanted mandibles were minimal, with a maximum difference of 1.15 MPa. The intact mandible of Model 2 and Model 3 showed the highest maximum principal stresses at 8.91 MPa and 8.94 MPa during intercuspal bites

and the lowest at 3.95 MPa and 4.14 MPa both occurring during LGF biting condition, respectively.

Molar bites (RMOL/LMOL) resulted in higher stress distribution in the mandible compared to group function bites. The peak magnitude of the principal stress (~19 MPa) was found in the lowest screw hole in the implanted mandibles in INC loading cases. In the full cortical model (Model 2), the principal stress in the cortical bone reached a peak value of 9.17 MPa in the narrow TMJ implant. A similar observation was made for Model 3 which reported a peak stress of 9.35 MPa in the narrow TMJ implant. The contour plots showed almost similar stress distribution in the human mandible under given loading conditions. There is a slight increment (between 0.1 – 1.15 MPa) in maximum principal stress values from Model 2 to the Model 3 except for the INC case in the intact mandible.

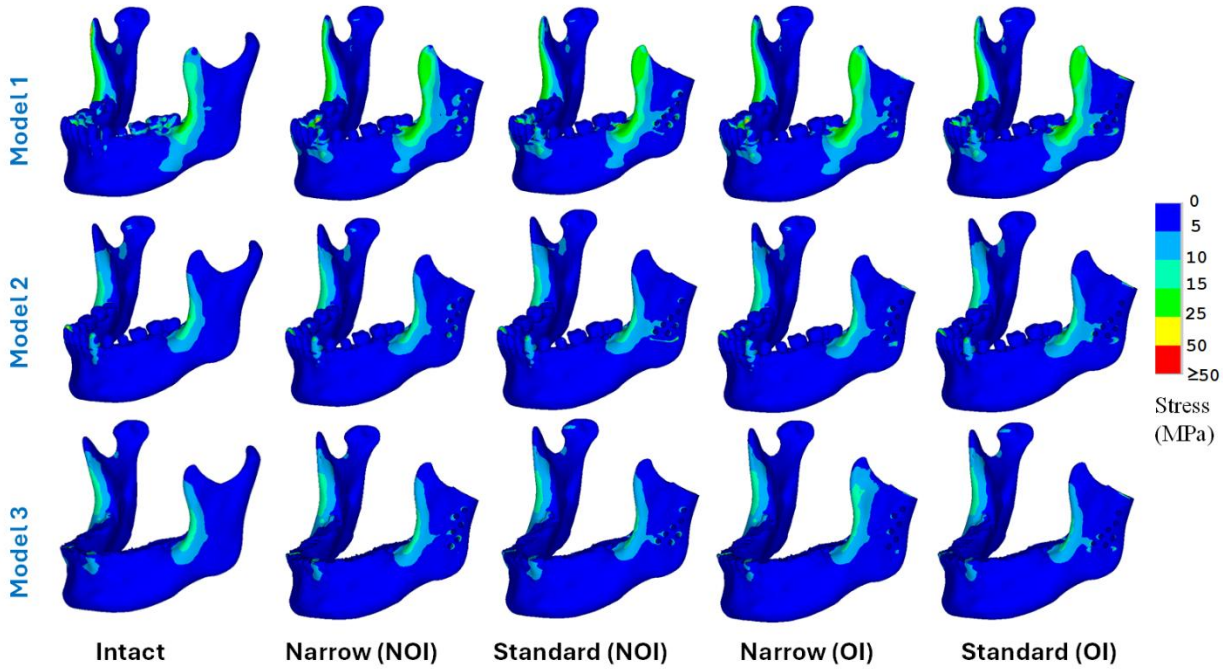

Figure 3. Comparison of maximum principal stress distribution on the cortical bone in various FE models (Model 1: Detailed Segmented Mandible, Model 2: Cortical Mandible, Model 3: Cortical mandible without crown of teeth, NOI: non-osseointegrated, OI: osseointegrated) under ICP bite

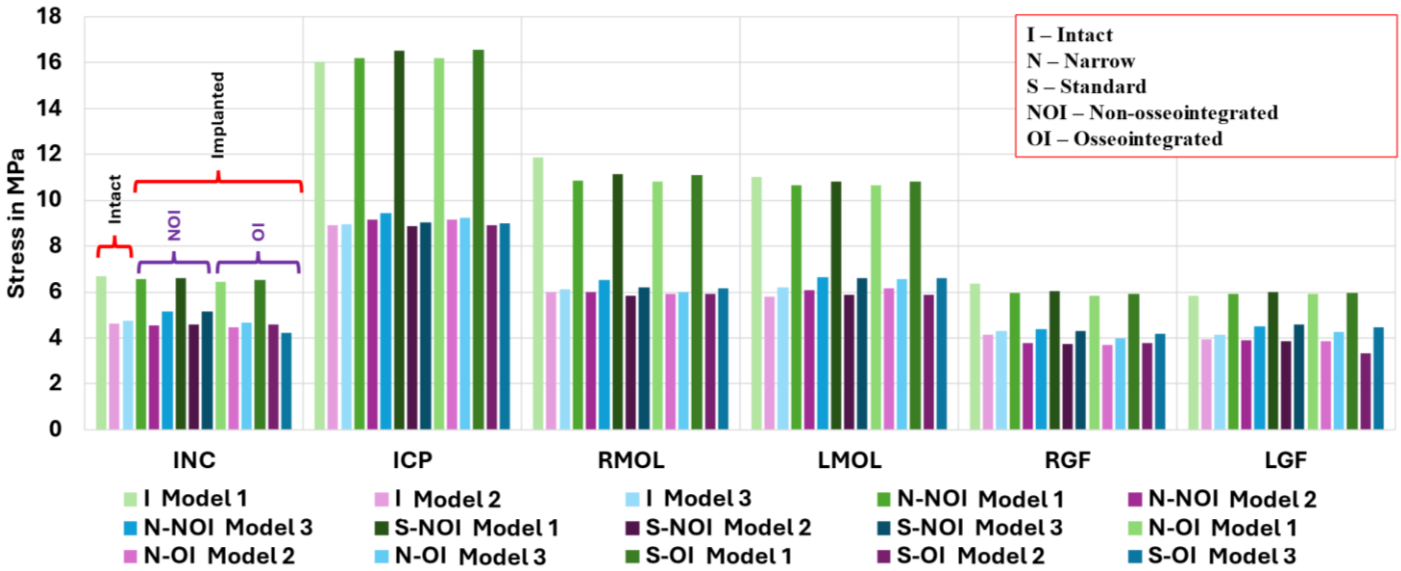

Figure 4. Maximum principal stress in the intact and implanted (with narrow/standard mandibular component) mandible for six clenching tasks in Model 1 (Ghosh et al., 2024) Model 2 and Model 3

3.1.2 Principal Strains on mandible

Figure 5 shows the principal strain distribution in intact as well as implanted mandibles (with narrow and standard mandibular components) under the ICP biting case due to observed higher severity than other biting cases from our previous study (Ghosh et al., 2024). All biting cases are shown in Appendix Figure 2 for principal strain distribution. The variation of principal strains in intact and implanted mandible was relatively large (Figure 5), and it was obtained in the range of 394 - 1040 με (Figure 6). The principal strain was also highest (max. 1040 με) in the case of ICP load case for Model 2 and Model 3 whereas the RGF/LGF load cases (min. 394 με) showed the lowest principal strain across different clenching tasks. The maximum values of strain were observed at the same location as the principal stresses, which is the lowest screw hole. There was a considerable difference in principal strain values (452-1050 με) and their distribution in the mandible in the ICP load case compared to other occlusions, with more extensive regions exposed

to higher strain. The symphyseal and mental region is the least affected region among the three zones of the full cortical mandible. High principal strains were majorly distributed on the posterior and gonial regions.

The worst-case scenario was observed during the intercuspal (ICP) bite which produced higher strains (Model 2: 920-994 με, Model 3: 970-1040 με) compared to other clenching tasks. The value of maximum principal strain was slightly higher (upto 136 με) in the Model 3 than in the Model 2. The difference between maximum principal strain values in implanted and intact was almost negligible (max. 95 με) in almost all loading cases.

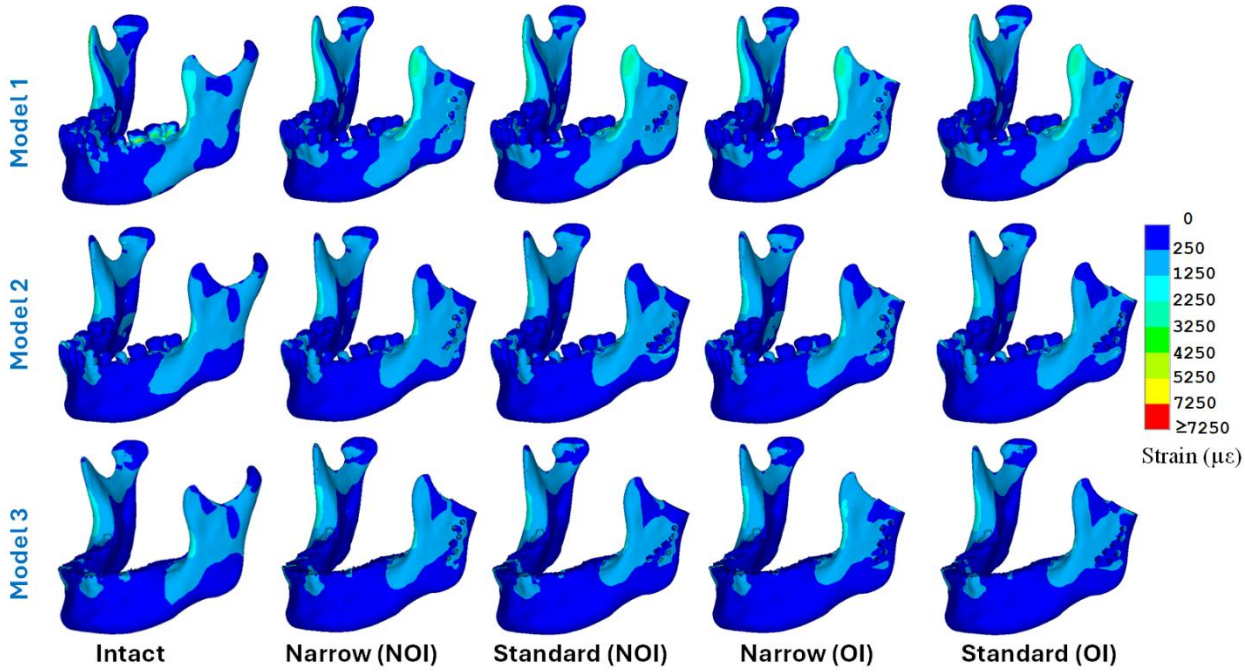

Figure 5. Comparison of maximum principal strain distribution on the cortical bone in various FE models (Model 1: Detailed Segmented Mandible, Model 2: Cortical Mandible, Model 3: Cortical mandible without crown of teeth, NOI: non-osseointegrated, OI: osseointegrated) under ICP bite

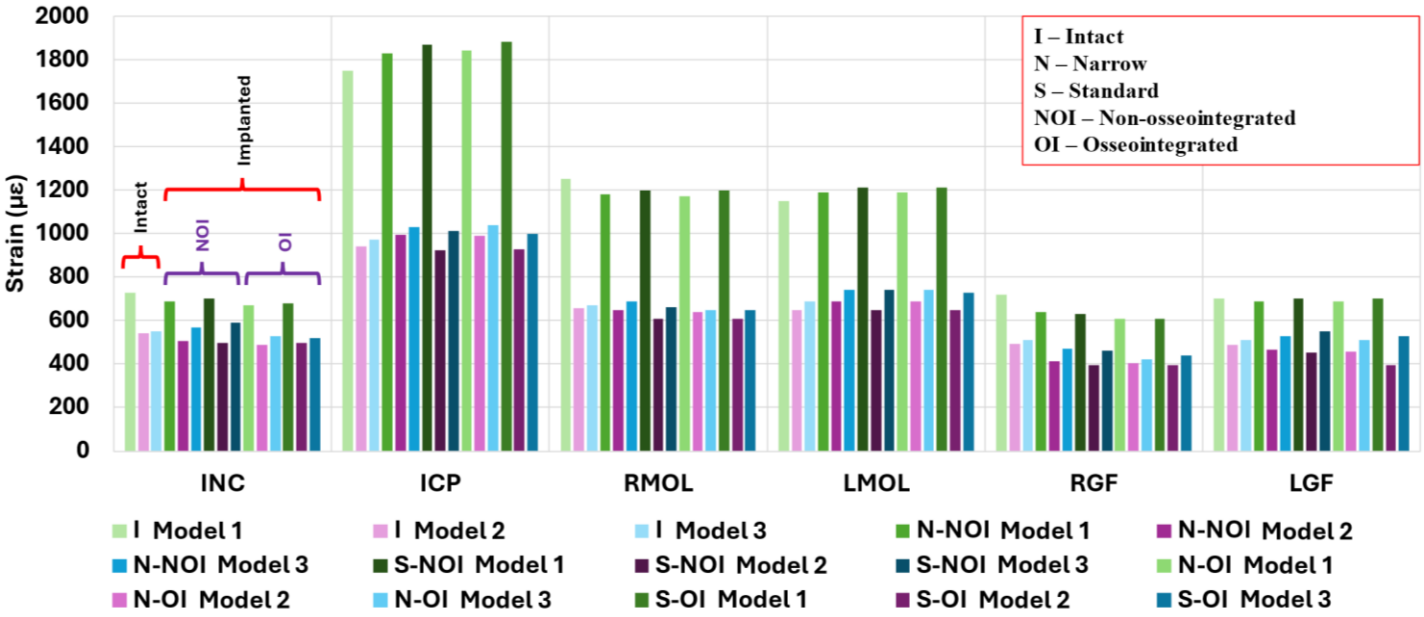

Figure 6. Maximum principal strain in the intact and implanted (with narrow/standard mandibular component) mandible for six clenching tasks (under complete mastication cycle) in Model 1 (Ghosh et al., 2024), Model 2 and Model 3

3.2 Stresses on TMJ Implants

Figures 7 (under ICP biting conditions due to observed higher severity than other biting cases from our previous study (Ghosh et al., 2024)) and 8 show the von Mises stress distribution and their values respectively in mandibular components and screws of TMJ implants. All biting cases are shown in Appendix Figure 3 for von-Mises stress distribution. For the mandibular component, the maximum von Mises stress in narrow mandibular component for each of the six clenching tasks ranged between 171.04 MPa in LMOL to 212.74 MPa in ICP. The maximum von Mises stress in screws ranged between 13.47 MPa in LMOL to 129.49 MPa in RGF across all models. The ICP and RMOL loadings were observed to be more intense across all models indicating the higher von Mises stress in implants. In the Model 2, the maximum stress in the mandibular component and

screws were 202.54 MPa and 109.94 MPa, whereas in the Model 3, the values changed to 212.74 MPa and 117.16 MPa, respectively. In all biting cases, the maximum von Mises stresses in TMJ implants were much less than the yield strength (~800 MPa) (Farooq et al., 2020) of Ti -alloy used in this study.

On comparing the peak values of von Mises stresses in implants obtained in Model 2 and Model 3, narrow TMJ showed higher stresses with Model 3 but not in Model 2 while conversely, standard TMJ showed overall higher stress with Model 2 but not in Model 3. The von Mises stress distribution in narrow and standard mandibular components along with the screws for each of six clenching tasks is shown in Figure 5. The contour plots showed a similarity in the stress distribution patterns for each load case in Model 2 and Model 3.

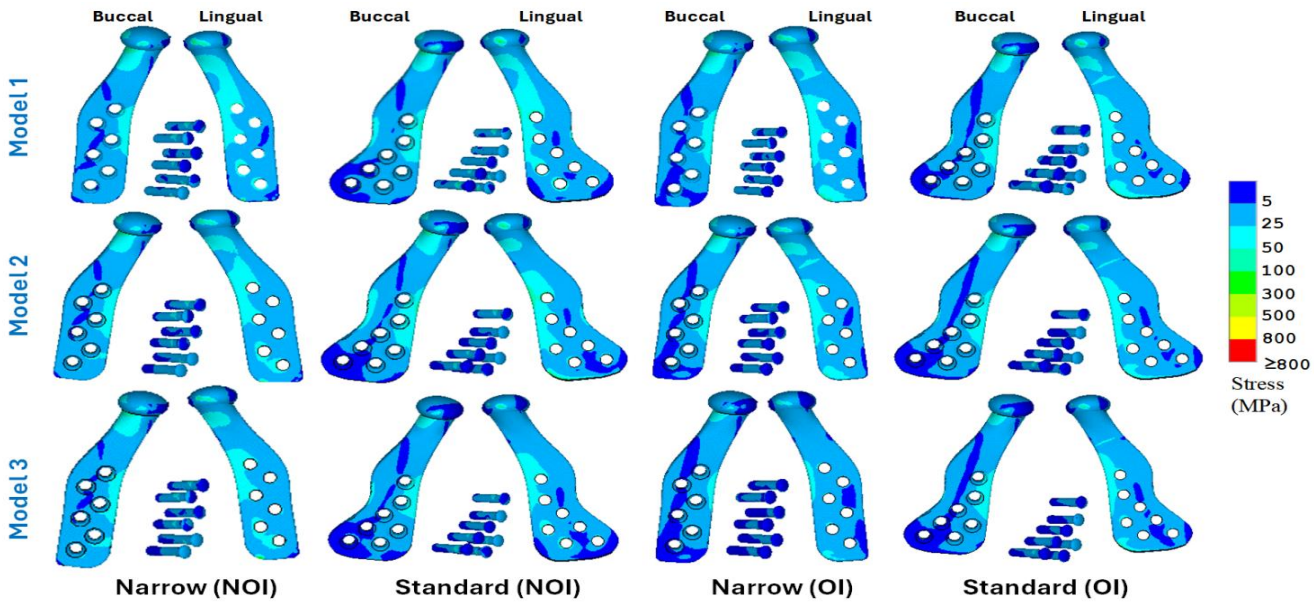

Figure 7. Comparison of maximum von Mises stress distribution on the implants (Mandibular component and Screws) in various FE models (Model 1: Detailed Segmented Mandible, Model 2: Cortical Mandible, Model 3: Cortical mandible without crown of teeth, NOI: non-osseointegrated, OI: osseointegrated) under ICP bite

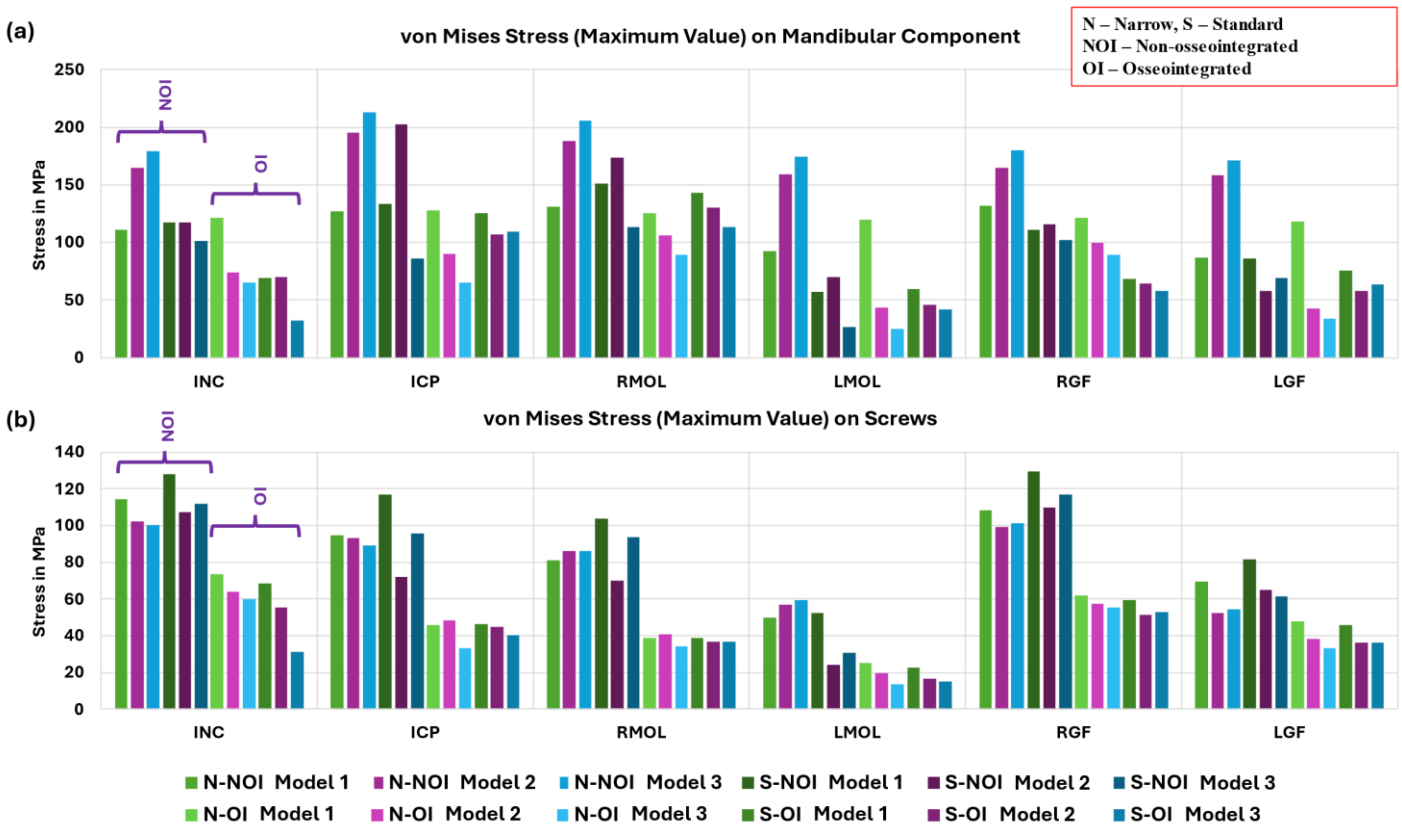

Figure 8. von Mises stresses (peak values) in (a) mandibular component and (b) screws for six clenching tasks in Model 1 (Ghosh et al., 2024), Model 2 and Model 3

3.3 Influence of osseointegration

This study also investigated the influence of bone-implant interface conditions considering non-osseointegrated (NOI) or frictional and osseointegrated (OI) or bonded conditions. The conditions at the bone-implant interface were found to influence the stresses (Figure 3) and strains (Figure 5) in the bone and implant. An osseointegrated condition reported an overall reduction in stress (narrow TMJ: 0.49 MPa; standard TMJ: 0.93 MPa) and strains (narrow TMJ: 50 $\mu\varepsilon$; standard TMJ: 70 $\mu\varepsilon$) in the mandible. However, compared to ipsilateral loading in the mandibular component, contralateral loading produced more stress in both the interface conditions conditions. The magnitude of von Mises stress in implants were lesser in OI conditions than in NOI conditions in

both Model 2 and Model 3, irrespective of the clenching tasks. The maximum von Mises stress in the NOI condition was 224.66 MPa, and which was reported 130.03 MPa in the OI condition across all models analyzed. The two different bone-implant interface conditions showed different trends for the Model 2 and Model 3. There is an overall reduction in von Mises stress (up to 149.03 MPa) in both implant types (standard and narrow) in the Model 2under OI conditions compared to the NOI condition. In addition, an overall reduction in stresses (up to 80.22 MPa) on the screws was also observed with both narrow and standard TMJ implants in the OI condition compared to the NOI condition. Overall, osseointegration reduces the stress and strain in mandible and TMJ implants under a full mastication cycle.

3.4 Influence of mandible simplification

To identify the influence of mandible simplification teeth mandible model on stresses and strains across mandible and implants, Models 2 and 3 of the present study were also compared with Model 1 from our previous study (Ghosh et al., 2024). Considering the ICP load case for intact mandibles, the maximum principal stresses obtained were 16.02 MPa for Model 1 (Ghosh et al., 2024), 8.91 MPa for Model 2, and 8.94 MPa for Model 3. The corresponding maximum principal strains were 1750 με (Ghosh et al., 2024), 939 με, and 970 με respectively. Almost similar principal stress and strain distributions were observed in the mandible for remaining clenching tasks (other than ICP) regardless of the implant and bone-implant interface condition. However, the distribution of principal stress and strain in the mandible of Model 2 and Model 3 showed an overall decrease compared to Model 1. Model 2 and Model 3 showed a respective reduction of 29-49% and 22-48% in maximum principal stress, and 25-50% and 16-47% reduction in maximum principal strain on cortical bone (across all biting cases) when compared with the Model 1. When the principal stress and strain results of cortical bone were compared between Model 2 and Model 3, it showed

lesser variation in intact models (up to 7%) than in implanted ones (up to 35%). The variation in maximum von Mises stresses was up to 62% for the mandibular component and up to 43% for the screws, between these two simplified models.

4. Discussion

The present study aims to evaluate the effect of material homogenization and anatomical simplification of the mandible on the biomechanical assessment of two commercially used mandibular TMJ implants under a mastication cycle. Additionally, influences of bone-implant interface conditions (based on level of osseointegration) on biomechanical characterization of mandible and performance of TMJ implants have also been investigated.

As usual, temporomandibular joint (TMJ) replacement systems are well-accepted final-stage treatment options for multiple TMJ disorders such as osteoarthritis, ankyloses, trauma, cancer, etc. Like any implantable device, TMJ implant designs should also be based on biomechanical principles and should reproduce the same function as observed in a healthy joint. The finite element analysis is used for the biomechanical assessment of these implants and involves some simplification strategies. An experimental study (Meyer et al., 2002) conducted on isolated mandible under RMOL bite showed the presence of tensile strains along the anterior border of the ramus and the condylar neck like the observation made in the presently developed FE models. The location of the highest principal strain around the oblique line in Model 2 and Model 3 (under INC, ICP, and molar bites) were also in corroboration with the earlier studies (Ghosh et al., 2024, Gröning et al., 2013). Compared to other biting conditions, the cortical bone during the intercuspal loading showed an extensive region of higher principal stress in the coronoid process and near the intercuspal region. This might be due to the bilateral constraints in intercuspal loading while the coronoid process is attached to the temporalis muscle responsible for the

elevation and retrusion of the mandible during mastication The finding that ICP produced the maximum stress and strain on cortical bone among all six clenching tasks was also consistent with the prior investigations (Hijazi et al., 2016; H. L. Huang et al., 2015).

Changes in the bone-implant interface condition (frictional to bonded) observed an overall reduction in stresses in the mandibular components and screws due to osseointegration in the bonded OI condition. Such a similar finding was also observed in an erstwhile study on dental implants (Niroomand & Arabbeiki, 2020). This finding might be attributed to the fact that screws act as load transferring intermediate mechanical components between mandible and mandibular component during the immediate post-operative or NOI condition due to interfacial movement. However, this interfacial movement is restricted during the long-term OI condition that reduces the load-sharing between the mandible and the mandibular component.

Other simplification made in this study was the consideration of homogenized material properties across the different biological tissues. To validate the results of FEA considering these assumptions, adequate reliability is required with confidence. The results from an earlier study on Model 1 (Ghosh et al., 2024) model are used for comparison and checking the accuracy of these two simplified cortical mandible models (Figure 4, 6 and 8). A major difference (up to ~ 50%) in stress and strain magnitude between the detailed and simplified mandible was observed in this study. Apart from this, this study also reported a huge difference in evaluated maximum (7.09 MPa for stress and 840 με for strain) and minimum (2.52 MPa for stress and 216 με for strain) values for stress and strains between the Model 1 and the simplified models. However, von Mises stress in mandibular components was found to be increased (up to 96.4%) with simplified implanted mandibles with narrow TMJ under NOI condition. On the contrary, the same was found to be overall decreased (up to 79%) in OI condition. However, overall reduction (up to 54%) in von

Mises stresses in screws were observed in simplified mandible with standard TMJ in both NOI and OI respectively.

The observed change in principal stress and strains in the cortical bone of the mandible from Model 1 to Model 2, and then Model 3, indicates the impact of simplification of reconstructed anatomical models and material homogenization. The Model 2 assumed cancellous bone, teeth, and periodontal ligament, all to be made of cortical bone, and hence assigned the three-zone wise orthotropic material properties of cortical bone. Of which, cancellous bone and periodontal ligament have significantly lower, and enamel and dentin have higher elastic modulus than the cortical bone. The high volume fraction of elements corresponding to the cancellous bone and periodontal ligament causes the rise in the overall stiffness of the mandible, and hence the reduction in principal stress and strain. Omitting the tooth structures resulted in a slight drop in its stiffness and hence a slight increase in the stress and strain values was observed. This change in consideration of material properties of the mandible in the present study was also responsible for the difference in von Mises stress of mandibular components and screws as obtained in an earlier study (Ghosh et al., 2024). Apart from these facts, the mechanical properties of cortical are chosen orthotropic which might differ according to various regions of the mandible from a maximum in the enamel region of teeth to a minimum in the PDL region. Since these mandible model simplifications have a larger effect on the simulation results, the material property-based assumptions should be made judiciously while performing the finite element investigations. In addition, due to these huge differences in results between detailed and simplified mandible and their TMJ implants that show unacceptable reality, the use of mandible simplification could be avoided for the prediction of the biomechanical behaviour.

5. Conclusion

The use of simplified models (Model 2 and Model 3) for biomechanical evaluation in finite element studies underestimated (by ~25-50%) the maximum principal stress and strain values in cortical bone. This significant change is caused by the simplicity of the cancellous, teeth, and periodontal ligaments, which led to stiffer cortical bone and ultimately increased the structure's overall stiffness. The maximum principal stress and strain in bone showed no significant dependence on the type of mandibular component, and bone-implant interface in the MODEL 1 model. Whereas Model 2 (in LGF loading) and Model 3 (in INC loading) showed different observations. The assumption of a full cortical mandible and omitting the tooth structures have significant alterations to the maximum stress and strain values but showed almost similar stress and strain distribution contours on the mandibular component. The overall reduction of principal stress and strain on bone was clearly visible in the Model 2 and Model 3 with respect to the Model 1. It suggests that, while simplified mandible models offered modeling, meshing, and computational advantages, they should not be used in future finite element simulation studies. This is because more detailed mandible models give more accurate results, and vice versa. The mandible model should incorporate all components and accurately assign the respective material properties to closely resemble the real scenario.

CRediT authorship contribution statement

Girish Chandra: Conceptualization, Data Curation, Formal Analysis, Investigation, Methodology, Validation, Visualization, Writing – original draft, Writing – review & editing. **Vivek Verma:** Data Curation, Formal Analysis, Investigation, Methodology, Visualization, Writing – original draft, Writing – review & editing. **Rajdeep Ghosh:** Conceptualization, Formal Analysis, Investigation, Methodology, Software, Visualization, Writing – review & editing. **Ajoy**

Roychoudhury: Funding acquisition, Project Administration, Resources, Supervision. **Sudipto Mukherjee:** Conceptualization, Funding acquisition, Methodology, Project Administration, Resources, Supervision, Writing – review & editing. **Anoop Chawla:** Conceptualization, Funding acquisition, Methodology, Project Administration, Resources, Supervision, Writing – review & editing. **Kaushik Mukherjee:** Conceptualization, Funding acquisition, Methodology, Project Administration, Resources, Supervision, Writing – review & editing.

Acknowledgments

The study was supported by the Indo–German Science & Technology Centre (IGSTC), under grant no. IGSTC/Call 2020/add-bite/48/2021-22/260.

Conflict of interest

There are no possible conflicts of interest for the authors in terms of funding support, research, authorship, or publishing of this paper.

References

Afzal, Z., & Warburton, G. (2019). Secondary Traumatic TMJ Reconstruction. In *Facial Trauma Surgery: From Primary Repair to Reconstruction*. Elsevier Inc. https://doi.org/10.1016/B978-0-323-49755-8.00044-X

Al-Ahmari, A., Nasr, E. A., Moiduddin, K., Anwar, S., Kindi, M. Al, & Kamrani, A. (2015). A comparative study on the customized design of mandibular reconstruction plates using finite element method. *Advances in Mechanical Engineering*, *7*(7), 1–11. https://doi.org/10.1177/1687814015593890

Alagarsamy, R., Roychoudhury, A., Bhutia, O., Lal, B., Yadav, R., & Bhalla, A. S. (2021).

Evaluation of fit feasibility of stock total joint replacement in temporomandibular joint ankylosis patients. *British Journal of Oral and Maxillofacial Surgery*, *59*(7), 792–797. https://doi.org/10.1016/j.bjoms.2020.11.016

Balon, P., Vesnaver, A., Kansky, A., Kočar, M., & Prodnik, L. (2019). Treatment of end stage temporomandibular joint disorder using a temporomandibular joint total prosthesis: The Slovenian experience. *Journal of Cranio-Maxillofacial Surgery*, *47*(1), 60–65. https://doi.org/10.1016/j.jcms.2018.10.022

Banerjee, A., Basu, B., Saha, S., & Chowdhury, A. R. (2023). Design and development of a patient-specific temporomandibular joint implant: Probing the influence of bone condition on biomechanical response. *Journal of Biomedical Materials Research - Part B Applied Biomaterials*, *July*, 1–9. https://doi.org/10.1002/jbm.b.35311

BIOMET Microfixation. (2007). *Mandibular Joint Replacement System by Zimmer Biomet*. https://doi.org/http://www.wlorenz.com.co/sites/default/files/documentos_producto/TMJ.pdf

Carrion, P. E., Shamsaei, N., Daniewicz, S. R., & Moser, R. D. (2017). Fatigue behavior of Ti-6Al-4V ELI including mean stress effects. *International Journal of Fatigue*, *99*, 87–100. https://doi.org/10.1016/j.ijfatigue.2017.02.013

Deshmukh, T. R., Kuthe, A. M., Chaware, S. M., Bagaria, V., & Ingole, D. S. (2012). A novel rapid prototyping and finite element method-based development of the patient-specific temporomandibular joint implant. *Computer Methods in Biomechanics and Biomedical Engineering*, *15*(4), 363–370. https://doi.org/10.1080/10255842.2010.538385

Dutta, A., Mukherjee, K., Seesala, V. S., Dutta, K., Paul, R. R., Dhara, S., & Gupta, S. (2023).

Comparative evaluation of a patient-specific customised plate designs and screws for partial mandibular reconstruction. *Medical Engineering and Physics*, *111*(September 2022), 103941. https://doi.org/10.1016/j.medengphy.2022.103941

Elledge, R., Mercuri, L. G., Attard, A., Green, J., & Speculand, B. (2019). Review of emerging temporomandibular joint total joint replacement systems. *British Journal of Oral and Maxillofacial Surgery*, *57*(8), 722–728. https://doi.org/10.1016/j.bjoms.2019.08.009

Fan, R., Liu, J., & Jia, Z. (2023). Biomechanical evaluation of different strain judging criteria on the prediction precision of cortical bone fracture simulation under compression. *Frontiers in Bioengineering and Biotechnology*, *11*(April), 1–9. https://doi.org/10.3389/fbioe.2023.1168783

Farooq, M. U., Mughal, M. P., Ahmed, N., Mufti, N. A., Al-Ahmari, A. M., & He, Y. (2020). On the investigation of surface integrity of Ti6Al4V ELI using si-mixed electric discharge machining. *Materials*, *13*(7). https://doi.org/10.3390/ma13071549

Filardi, V. (2020). Stress shielding FE analysis on the temporomandibular joint. *Journal of Orthopaedics*, *18*(September 2019), 63–68. https://doi.org/10.1016/j.jor.2019.09.013

Ghosh, R., Chandra, G., Verma, V., Kaur, K., & Roychoudhury, A. (2024). Biomechanical Evaluation of Temporomandibular Joint Implants Under. *BioRxiv*. https://doi.org/https://doi.org/10.1101/2024.08.26.609607

Gonzalez-Perez, L. M., Gonzalez-Perez-Somarriba, B., Centeno, G., Vallellano, C., Montes-Carmona, J. F., Torres-Carranza, E., Ambrosiani-Fernandez, J., & Infante-Cossio, P. (2020). Prospective study of five-year outcomes and postoperative complications after total temporomandibular joint replacement with two stock prosthetic systems. *British Journal of*

Oral and Maxillofacial Surgery, *58*(1), 69–74. https://doi.org/10.1016/j.bjoms.2019.10.312

Hijazi, L., Hejazi, W., Darwich, M. A., & Darwich, K. (2016). Finite element analysis of stress distribution on the mandible and condylar fracture osteosynthesis during various clenching tasks. *Oral and Maxillofacial Surgery*, *20*(4), 359–367. https://doi.org/10.1007/s10006-016-0573-2

Huang, C. M., Chan, M. Y., Hsu, J. T., & Su, K. C. (2021). Biomechanical analysis of subcondylar fracture fixation using miniplates at different positions and of different lengths. *BMC Oral Health*, *21*(1), 1–12. https://doi.org/10.1186/s12903-021-01905-5

Huang, H. L., Su, K. C., Fuh, L. J., Chen, M. Y. C., Wu, J., Tsai, M. T., & Hsu, J. T. (2015). Biomechanical analysis of a temporomandibular joint condylar prosthesis during various clenching tasks. *Journal of Cranio-Maxillofacial Surgery*, *43*(7), 1194–1201. https://doi.org/10.1016/j.jcms.2015.04.016

Ingawalé, S., & Goswami, T. (2009). Temporomandibular joint: Disorders, treatments, and biomechanics. *Annals of Biomedical Engineering*, *37*(5), 976–996. https://doi.org/10.1007/s10439-009-9659-4

Ingawale, S. M., & Goswami, T. (2022). Design and Finite Element Analysis of Patient-Specific Total Temporomandibular Joint Implants. *Materials*, *15*(12). https://doi.org/10.3390/ma15124342

Kashi, A., Chowdhury, A. R., & Saha, S. (2010). Finite element analysis of a TMJ implant. *Journal of Dental Research*, *89*(3), 241–245. https://doi.org/10.1177/0022034509357716

Keyser, B. R., Banda, A. K., Mercuri, L. G., Warburton, G., & Sullivan, S. M. (2020).

Alloplastic total temporomandibular joint replacement in skeletally immature patients: a pilot survey. *International Journal of Oral and Maxillofacial Surgery*, *49*(9), 1202–1209. https://doi.org/10.1016/j.ijom.2020.02.001

Kharmanda, G., & Kharma, M. Y. (2017). Evaluating the Effect of Minimizing Screws on Stabilization of Symphysis Mandibular Fracture by 3D Finite Element Analysis. *Journal of Maxillofacial and Oral Surgery*, *16*(2), 205–211. https://doi.org/10.1007/s12663-016-0903-9

Kim, M. R., & Donoff, R. B. (1992). Critical analysis of mandibular reconstruction using AO reconstruction plates. *Journal of Oral and Maxillofacial Surgery*, *50*(11), 1152–1157. https://doi.org/10.1016/0278-2391(92)90145-P

Korioth, T. W. P., Romilly, D. P., & Hannam, A. G. (1992). Three-dimensional finite element stress analysis of the dentate human mandible. *American Journal of Physical Anthropology*, *88*(1), 69–96. https://doi.org/10.1002/ajpa.1330880107

Luo, D., Rong, Q., & Chen, Q. (2017). Finite-element design and optimization of a three-dimensional tetrahedral porous titanium scaffold for the reconstruction of mandibular defects. *Medical Engineering and Physics*, *47*, 176–183. https://doi.org/10.1016/j.medengphy.2017.06.015

Mesnard, M., Ramos, A., Ballu, A., Morlier, J., Cid, M., & Simoes, J. A. (2011). Biomechanical analysis comparing natural and alloplastic temporomandibular joint replacement using a finite element model. *Journal of Oral and Maxillofacial Surgery*, *69*(4), 1008–1017. https://doi.org/10.1016/j.joms.2010.02.019

Nakhaei, M., Sterba, M., Foletti, J. M., Badih, L., & Behr, M. (2023). Experimental analysis and

numerical fatigue life prediction of 3D-Printed osteosynthesis plates. *Frontiers in Bioengineering and Biotechnology*, *11*(March), 1–13. https://doi.org/10.3389/fbioe.2023.1133869

Niroomand, M. R., & Arabbeiki, M. (2020). Implant stability in different implantation stages: Analysis of various interface conditions. *Informatics in Medicine Unlocked*, *19*, 100317. https://doi.org/10.1016/j.imu.2020.100317

Oguz, Y., Uckan, S., Ozden, A. U., Uckan, E., & Eser, A. (2009). Stability of locking and conventional 2.0-mm miniplate/screw systems after sagittal split ramus osteotomy: finite element analysis. *Oral Surgery, Oral Medicine, Oral Pathology, Oral Radiology and Endodontology*, *108*(2), 174–177. https://doi.org/10.1016/j.tripleo.2009.03.051

Pinheiro, M., Willaert, R., Khan, A., Krairi, A., & Van Paepegem, W. (2021). Biomechanical evaluation of the human mandible after temporomandibular joint replacement under different biting conditions. *Scientific Reports*, *11*(1), 1–12. https://doi.org/10.1038/s41598-021-93564-3

Schileo, E., Dall'Ara, E., Taddei, F., Malandrino, A., Schotkamp, T., Baleani, M., & Viceconti, M. (2008). An accurate estimation of bone density improves the accuracy of subject-specific finite element models. *Journal of Biomechanics*, *41*(11), 2483–2491. https://doi.org/10.1016/j.jbiomech.2008.05.017

Seol, G.-J., Jeon, E.-G., Lee, J.-S., Choi, S.-Y., Kim, J.-W., Kwon, T.-G., & Paeng, J.-Y. (2014). Reconstruction plates used in the surgery for mandibular discontinuity defect. *Journal of the Korean Association of Oral and Maxillofacial Surgeons*, *40*(6), 266. https://doi.org/10.5125/jkaoms.2014.40.6.266

Vignesh, U., Mehrotra, D., Bhave, S. M., Katrolia, R., & Sharma, S. (2020). Finite element analysis of patient-specific TMJ implants to replace bilateral joints with simultaneous correction of facial deformity. *Journal of Oral Biology and Craniofacial Research*, *10*(4), 674–679. https://doi.org/10.1016/j.jobcr.2020.07.013

Wang, R., Liu, Y., Wang, J. H., & Baur, D. A. (2017). Effect of interfragmentary gap on the mechanical behavior of mandibular angle fracture with three fixation designs: A finite element analysis. *Journal of Plastic, Reconstructive and Aesthetic Surgery*, *70*(3), 360–369. https://doi.org/10.1016/j.bjps.2016.10.026

Yoda, T., Ogi, N., Yoshitake, H., Kawakami, T., Takagi, R., Murakami, K., Yuasa, H., Kondoh, T., Tei, K., & Kurita, K. (2020). Clinical guidelines for total temporomandibular joint replacement. *Japanese Dental Science Review*, *56*(1), 77–83. https://doi.org/10.1016/j.jdsr.2020.03.001